

Experimental Quantum State Tomography via Compressed Sampling

Wei-Tao Liu,^{1,*} Ting Zhang,¹ Ji-Ying Liu,² Ping-Xing Chen,¹ and Jian-Min Yuan¹

¹*Department of Physics, College of Science, National University of Defense Technology, Changsha, 410073, People's Republic of China*

²*Department of Mathematics and Systems Science, College of Science, National University of Defense Technology, Changsha, 410073, People's Republic of China*

(Received 2 September 2011; published 24 April 2012)

A fundamental difficulty in demonstrating quantum state tomography is that the required resources grow exponentially with the system size. For pure states and nearly pure states, the task of tomography can be more efficient. We proposed two methods for state reconstruction, by (1) minimizing entropy and (2) maximizing likelihood. The algorithm of compressed sampling is employed to solve the optimization problem. Experiments are demonstrated considering 4-qubit photonic states. The results show that (1) much fewer measurements than the standard tomography are sufficient to obtain high fidelity, and (2) the method of maximizing likelihood is more accurate and noise robust than the original reconstruction method of compressed sampling. Furthermore, the physical meaning of the methods of minimizing entropy and maximizing likelihood is clear.

DOI: 10.1103/PhysRevLett.108.170403

PACS numbers: 03.65.Wj, 03.65.Yz, 03.67.Lx

Quantum state tomography and quantum process tomography are essential tasks in physics, especially in quantum information science [1]. Although standard tomography methods have been developed and demonstrated for qubit systems, there is a fundamental difficulty. That is, the required resources grow exponentially with the dimension of the state space. Considering a d -dimensioned system, $N = d^2$ measurements are necessary for state tomography and $N = d^4$ experimental configurations for process tomography, with the standard method. Additionally, to obtain high precision, each measurement has to be repeated many times, say M . So that $N \times M$ copies of such physical states (the input states may be different for process tomography) are necessary. Whereafter, postprocessing of large data also consumes many resources. Recently, efficient quantum tomography of multiqubit states and processes has drawn a lot of interest [2–9].

Fortunately, we are often interested in states and processes with special properties, such as pure states, ground states of a local Hamiltonian, unitary transformations, etc. Taking the properties of states and processes as *prior* knowledge, some measurements might be unnecessary; therefore, tomography in such special cases can be more efficient. Considering the problem of state reconstruction from measurements fewer than d^2 , the standard method will not work anymore, since there might be many solutions. In fact, prior knowledge of the considered states and the measured data can be treated as constraints that confine the density matrix within a certain ensemble. We can select the closest one to the real state within such an ensemble in an optimal way.

In this Letter, we proposed two methods for efficient tomography of pure or nearly pure states, by minimizing entropy or maximizing likelihood. The task of state reconstruction turns out to be an optimization problem similar to

those problems solved via compressed sampling (CS) [10–12], so we employ the algorithm of CS to solve the optimization problem. Experiments and numerical simulations are demonstrated on photonic states. By minimizing entropy or maximizing likelihood, the density matrix can be reconstructed with high fidelity from much fewer measurements, compared to the standard tomography method. Furthermore, the method of maximizing likelihood is more accurate and robust under statistical noise; thus, the number of required copies for each measurement can also be lower. Our approaches will be applicable for quantum tomography of large-scale quantum states and quantum processes. We also discuss the physical meaning of our approaches, which will be helpful for understanding the physics of CS.

CS provides methods for reconstructing a large-size sparse signal from a significant smaller one with efficient convex optimization algorithms. Sparsity here means that the number of nonzero entries of the signal vector is very small in a specified basis, and the measurements are linear functions of its entries. From a small number of randomly chosen measurements, the vector can be recovered with high probability. This method has been experimentally applied to ghost imaging [13–15], an efficient measurement of quantum dynamics [7]. Quantum state tomography for low-rank density matrices has also been discussed [8,9]. Suppose the density matrix is sparse, or it is close to a matrix of rank r , where r is very small, $O(rd)$ measurements could suffice for tomography on a d -dimension system [8]. It can be reconstructed by solving for ρ from the following convex optimization problem [8]:

$$\min \|\rho\|_{\text{tr}}, \quad \text{s.t. } \text{tr} \rho = 1, \quad \text{tr}(A_i \rho) = b_i, \quad (1)$$

where $\|\cdot\|_{\text{tr}} = \sum_j s_j$, with s_j being the singular values of the matrix, and A_i is a randomly chosen measurement

operator, with b_i being the corresponding measurement result. The number of randomly chosen A_i is of the order $m = O(rd)$. Considering the influence of noise, the problem in Eq. (1) should be replaced with [8]

$$\min \|\rho\|_{\text{tr}}, \quad \text{s.t.} \sum_{i=1}^m [\text{tr}(A_i \rho) - b_i]^2 \leq \varepsilon, \quad (2)$$

with ε being a positive parameter determined by estimating errors of the experimental data.

However, the physics of compressed sampling, even the physical meaning of the objective function employed in the reconstruction algorithm of Eq. (2), is unclear. The reconstructed matrix is confined within a convex set of the density matrices by the constraint in Eq. (2) and the objective function offers a criterion on how to select the very matrix, with its physical meaning unclear.

We propose two methods for state reconstruction, the objective functions of which are physically meaningful. Experimentally, all the statistical errors in measurements can be treated as random decoherence noise which tends to lead an expected state to appear less pure. Therefore, the constraint in Eq. (2) spans a convex ensemble in which the matrices are most likely not as pure as the real state. Or, the entropy of most density matrices contained in the ensemble are higher than the real state. Based on the prior information that the considered states are of low entropy, it is reasonable to find the one that is of lowest entropy and take it as the solution. Therefore, we take the entropy of ρ as an objective function of the optimization problem. That is, modify Eq. (2) into the following

$$\min -\text{tr}(\rho \log \rho), \quad \text{s.t.} \sum_{i=1}^m [\text{tr}(A_i \rho) - b_i]^2 \leq \varepsilon. \quad (3)$$

Besides, the probability that the reconstructed density matrix ρ could produce the measured data can be employed to qualify how good ρ is in relation to the experimental data. The higher the probability is, the closer to the real state is ρ . Therefore, such probability should be maximized, which is the main idea of maximum-likelihood estimation. Under the assumption that the noise on the measured counts has a Gaussian probability distribution, the task of maximizing the likelihood turns into minimizing the following function [16]

$$f(\rho) = M_0 \sum_{i=1}^m \frac{[\text{tr}(A_i \rho) - b_i]^2}{2 \text{tr}(A_i \rho)}, \quad (4)$$

with M_0 being the total number of copies used for each measurement. Taking M_0 as a constant, we get the following minimization problem for state reconstruction

$$\min \sum_{i=1}^m \frac{[\text{tr}(A_i \rho) - b_i]^2}{2 \text{tr}(A_i \rho)}, \quad \text{s.t.} \rho^\dagger = \rho, \quad \rho \geq 0, \quad \text{tr} \rho = 1. \quad (5)$$

The constraint here is introduced to ensure the reconstructed ρ is Hermitian, non-negative, and normalized. When using complete measurements, Eq. (5) turns out to be the standard tomography via maximum-likelihood estimation.

To validate our approaches, we perform an experimental demonstration and numerical simulations. For comparison, the original algorithm shown in Eq. (2) proposed in Ref [8] is also implemented. The experiments are demonstrated by estimating the density matrix of a photonic n -qubit system, with n chosen to be 2, 3, 4. The experimental setup is shown in Fig. 1. Two-photon polarization entangled states created via spontaneous parametric down-conversion are employed to prepare all the states. For 3- and 4-qubit states, the techniques of one-photon two-qubit are employed for the states' preparation and measurements [3,17]. The polarization and paths of the photon that go through the polarization beam splitter (PBS in Fig. 1) are encoded as the 1st and 2nd qubit, while those of the photon that go through the beam splitter (BS in Fig. 1) are encoded as the 3rd and 4th qubit. For comparison, we first performed standard quantum state tomography. On each qubit, each measurement is chosen from

$$\begin{aligned} \hat{\mu}_0 &= |0\rangle\langle 0|, & \hat{\mu}_1 &= |1\rangle\langle 1| \\ \hat{\mu}_2 &= |+\rangle\langle +|, & \hat{\mu}_3 &= |+i\rangle\langle +i|, \end{aligned} \quad (6)$$

where $|\pm\rangle = (|0\rangle \pm |1\rangle)/\sqrt{2}$ and $| \pm i \rangle = (|0\rangle \pm i|1\rangle)/\sqrt{2}$. For each n -qubit state, the complete set $\{A_i = \otimes_{j=1}^n \hat{\mu}_{k_j}^{(j)}\}$ of all the 4^n combinations of those four observables, with $\hat{\mu}_{k_j}^{(j)}$ being one of the four measurements on the j th qubit, is measured. Two Sagnac interferometers with high visibility and stability are constructed to perform measurements on the superposition state (namely, $\hat{\mu}_2$ and $\hat{\mu}_3$) of the path qubit. For the convenience of the experiments, the measurements are replaced with modified Bell state measurements [3] on the single-photon two-qubit state encoded in

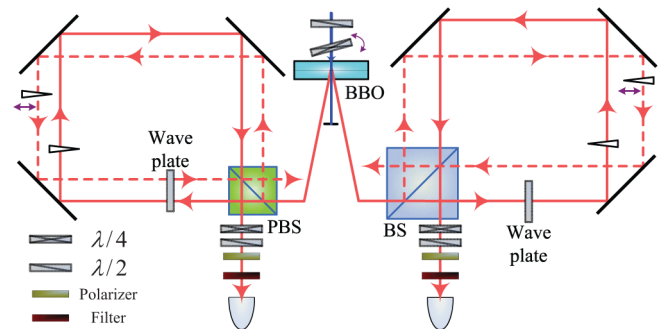


FIG. 1 (color online). Setup for the preparation and measurements of two-photon four-qubit states. Two-qubit states are prepared on the polarization states of twin photons created via spontaneous parametric down-conversion. Two interferometers are employed for preparing and measuring the path qubit. For three-qubit states, one of the interferometers is removed.

qubit 1 and 2, for those measurement operators containing $\hat{\mu}_2$ or $\hat{\mu}_3$ on the 2nd qubit. Based on the measured data, the density matrix ρ_S of each state is reconstructed with the standard method.

Then we implement the methods of reconstruction from fewer measurements. For each state, m different A_i s and corresponding measurement results b_i s are randomly chosen from the complete data set. The measurement error bound ε in Eq. (2) is chosen to be slightly larger than $\sum_{i=1}^m \sigma_i^2$, where σ_i is the standard deviation of b_i . Then the density matrix $\rho_m^{(2)}$ is reconstructed by solving Eq. (2). The density matrix reconstructed from the complete measurement data (all the 4^n measurements are used) $\rho_C^{(2)}$ is also calculated. Fidelity between ρ_S and $\rho_C^{(2)}$, as well as the fidelity between $\rho_m^{(2)}$ and $\rho_C^{(2)}$ are shown in Fig. 2 as squares. From top to bottom, the results for 2-, 3-, and 4-qubit states are shown. The error bars are obtained by solving Eq. (2) for 7 states and 10 different combinations of m measurements for each state.

By solving Eq. (3) and Eq. (5) with randomly chosen m measurements, the density matrices are also calculated. Fidelity between matrix $\rho_m^{(3)}$ ($\rho_m^{(5)}$) reconstructed from m measurements and $\rho_C^{(3)}$ ($\rho_C^{(5)}$) from 4^n measurements are

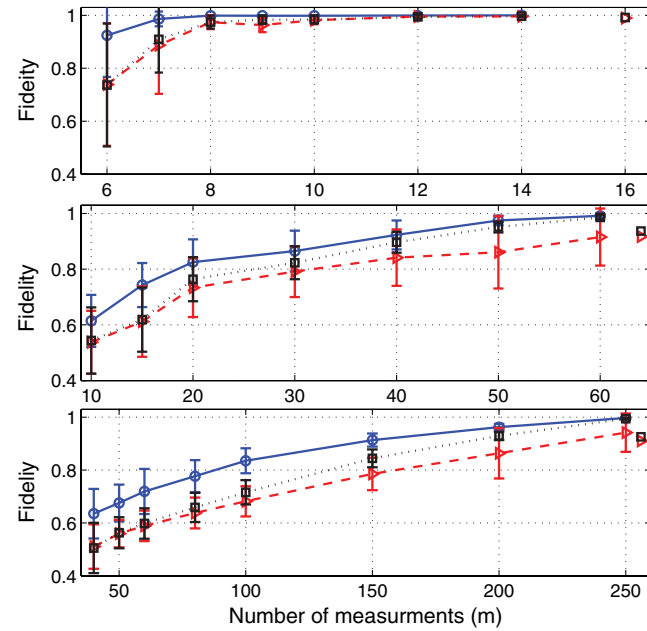


FIG. 2 (color online). Results of state tomography via compressed sampling. From top to bottom, results for 2-, 3- and 4-qubit are shown. For $m < 4^n$, fidelities between ρ_m reconstructed from m measurements and ρ_C from complete measurements are plotted. For $m = 4^n$, the dots show fidelities between ρ_C and ρ_S calculated with the standard method. Circles represent the results of solving Eq. (5), triangles for that of Eq. (3), and squares for Eq. (2). Error bars are obtained by solving those problems for 7 states and 10 different random chosen combinations of m measurements for each state.

shown in Fig. 2. The fidelity between ρ_S and $\rho_C^{(3)}$ ($\rho_C^{(5)}$) is also shown. In Fig. 2, the results of Eq. (3) are represented as triangles and that of Eq. (5) as circles.

As shown in Fig. 2, the reconstructed density matrices show high fidelities with the results of standard state tomography. At the same time, results of each algorithm show good consistency, and the results of three algorithms agree well, especially for 2-qubit states. For 3- and 4-qubit states, fidelities obtained are a little lower than that of 2-qubit. This is mainly caused by noise. On the one hand, b_i 's are calculated from coincidence counts. For 3- and 4-qubit states, the coincidence count rate gets lower due to higher loss in the experiments; therefore, statistical errors lead to higher relative errors. On the other hand, the expected states are changed into mixed states due to the phase errors in the interferometers. For each measurement that contains $\hat{\mu}_2$ or $\hat{\mu}_3$ on the path qubit, the phase of interferometers is set by observing the interference, the precision of which is dependent on the count rate. When the count rate decreases, the precision of the phase will also decrease. These kinds of errors can be treated as systematical noise introducing decoherence to the expected states; therefore, the rank of measured states gets higher, which makes the number of required measurements become larger for using compressed sampling.

To illustrate the performance of our methods for states of different purities under different levels of noise, we do some numerical simulations. The noiseless cases are first considered. Density matrices of different rank r and purity P are randomly produced for calculation. The results for $\{r = 1, P = 1\}$, $\{r = 2, P = 0.6\}$ and $\{r = 3, P = 0.38\}$ are shown in Fig. 3. For states of higher rank or lower purity, more measurements are required to obtain a certain

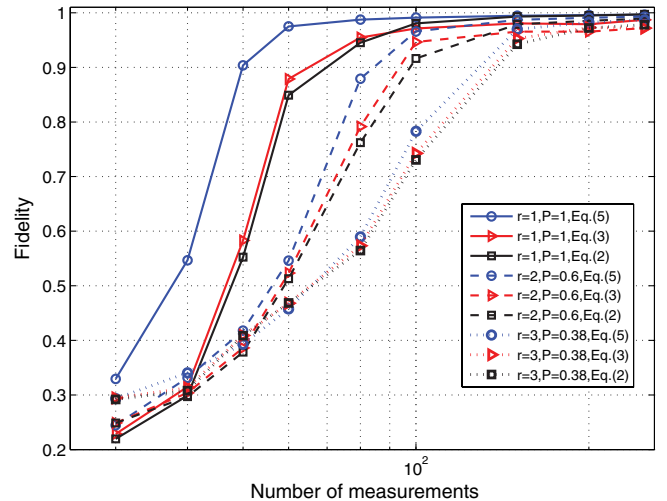


FIG. 3 (color online). Numerical results of compressed sampling based state tomography on 4-qubit states of rank r and purity P , without noise. The fidelities of matrices reconstructed from m measurements are shown. Circles represent results of Eq. (5), triangles for Eq. (3), and squares for Eq. (2).

level of fidelity. All the three algorithms can get high fidelity given enough measurement data without noise. About $(3rd)$ measurements are sufficient for reconstructing the density matrix with a fidelity higher than 0.9. For states of low rank, the number of required measurements is much lower than d^2 .

Then the cases with noise are considered. For each 4-qubit state ρ_e , the measurement data $\{b_i\}$ are produced by calculating $\text{tr}(\rho_e A_i)$ then adding Gaussian statistical noise on the coincidence count, with the standard deviation of b_i being $\sigma_i = \sqrt{M_0 \text{tr}(\rho_e A_i)}/M_0$, where M_0 is the total number of copies used for each measurement. The results of $\{r=2, P=0.98\}$, $\{r=2, P=0.6\}$ and $\{r=3, P=0.38\}$ with $M_0 = \{7000, 1000, 500\}$ are shown in Fig. 4. For pure or nearly pure states, all three algorithms are not very sensitive to statistical errors. $\sim 3rd$ measurements are still sufficient for high fidelity reconstruction. When the measured states are not so pure, the reconstruction algorithms become more sensitive to statistical errors. Especially, the fidelities of results from Eq. (3) become lower for less pure states than that of the other two algorithms, which imply that the algorithm of minimizing entropy is less effective for less pure states.

The experimental and numerical results show that, for pure states or nearly pure states, our methods can work

well and the number of required measurements N is of the order $O(rd)$. $\sim 3rd$ measurements are sufficient for reconstructing the density matrix with a fidelity higher than 0.9. Even when the number of copies M used for each measurement is rather low, the reconstructed matrix can obtain high fidelity. Therefore the total number of copies consumed for state tomography can be greatly cut down. From all these results, we find that the results of solving Eq. (5), or maximizing likelihood based on CS, perform a little better than the other two algorithms under the assumption of Gaussian statistical noise. That is, the method of maximizing likelihood is more accurate and noise robust, thus more practical than the other two.

Equations (3) and (5) show clear physical meaning. By solving Eq. (3), the density matrix is reconstructed by finding out the matrix of the lowest entropy, within an ensemble for all the states in which the errors between the expectation values and the measured data are lower than an error bound defined by ε , based on the prior information that the measured state is of low entropy. By solving Eq. (5), the density matrix is reconstructed by finding out the matrix that could produce the measured data with the highest probability, within the whole state space. In addition, the results of Eq. (3) are very close to that of Eq. (2) in most cases, which will be a hint for understanding the physics of Eq. (2).

Our results and algorithms can be generalized into large-scale systems, where the advantage of compressed sampling will be more prominent and helpful. Based on our results, efficient tomography of a multiqubit system becomes realizable, which will boost the development of experimental research in quantum physics. Our discussions about the physical meaning will be helpful for understanding the physics of CS.

Since the property of the representation matrix for unitary dynamics is very similar to that of pure state, tomography via CS discussed here can also be applied to tomography of quantum dynamics that can be expressed as unitary operations or nearly unitary ones. Although the reconstruction algorithms in Eqs. (3) and (5) have been experimentally demonstrated, mathematical proof is still expected. Further discussions on their application in practical experiments will also be helpful, such as the influence of other kinds of noise, the method to determine the error bound ε , etc.

This work is supported by the National Natural Science Foundation of China under Grants No. 11004248 and No. 10774192.

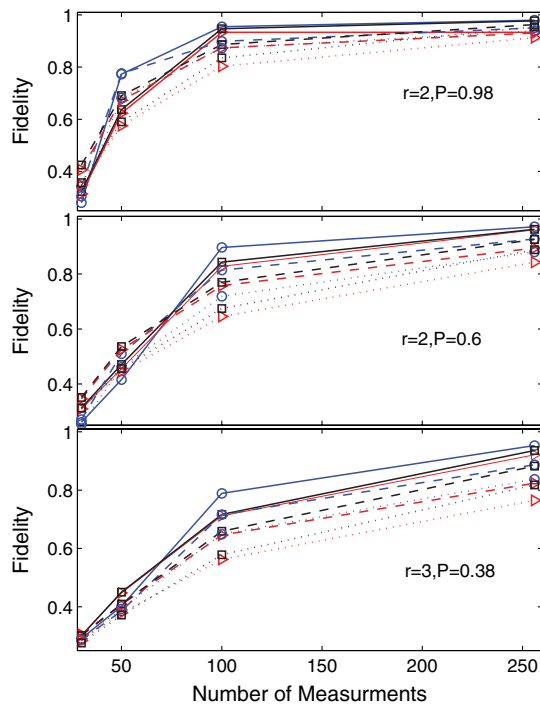


FIG. 4 (color online). Numerical results of compressed sampling based state tomography on 4-qubit states of rank r and purity P , under Gaussian noise. The fidelities of matrices reconstructed from m measurements are shown. Circles represent results of Eq. (5), triangles for Eq. (3), and squares for Eq. (2). Points on the solid lines are obtained with $M_0 = 7000$, dashed lines $M_0 = 1000$, and dotted lines $M_0 = 500$.

*wtliu@nudt.edu.cn

- [1] M. A. Nielsen and I. L. Chuang, *Quantum Computation and Quantum Information* (Cambridge University Press, Cambridge, England, 2000).

- [2] M. Mohseni and D. A. Lidar, *Phys. Rev. Lett.* **97**, 170501 (2006).
- [3] W. T. Liu, W. Wu, P. X. Chen, C. Z. Li, and J. M. Yuan, *Phys. Rev. A* **77**, 032328 (2008).
- [4] G. Tóth, W. Wieczorek, D. Gross, R. Krischek, C. Schwemmer, and H. Weinfurter, *Phys. Rev. Lett.* **105**, 250403 (2010).
- [5] S. T. Flammia and Y-K Liu, *Phys. Rev. Lett.* **106**, 230501 (2011).
- [6] C. T. Schmiegelow, A. Bendersky, M. A. Larotonda, and J. P. Paz, *Phys. Rev. Lett.* **107**, 100502 (2011).
- [7] A. Shabani, R. L. Kosut, M. Mohseni, H. Rabitz, M. A. Broome, M. P. Almeida, A. Fedrizzi, and A. G. White, *Phys. Rev. Lett.* **106**, 100401 (2011).
- [8] D. Gross, Y-K Liu, S. T. Flammia, S. Becker, and J. Eisert, *Phys. Rev. Lett.* **105**, 150401 (2010).
- [9] M. Cramer, M. Plenio, S. Flammia, R. Somma, D. Gross, S. Bartlett, O. Landon-Cardinal, D. Poulin, and Y.-K. Liu, *Nature Commun.* **1**, 149 (2010).
- [10] D. Donoho, *IEEE Trans. Inf. Theory* **52**, 1289 (2006).
- [11] E. Candès and T. Tao, *IEEE Trans. Inf. Theory* **52**, 5406 (2006).
- [12] E. Candès and M. Wakin, *IEEE Signal Process. Mag.* **25**, 21 (2008).
- [13] O. Katz, Y. Bromberg, and Y. Silberberg, *Appl. Phys. Lett.* **95**, 131110 (2009).
- [14] J. Y. Liu, J. B. Zhu, C. Lu, and S. S. Huang, *Opt. Lett.* **35**, 1206 (2010).
- [15] W. L. Gong and S. S. Han, [arXiv:0910.4823](https://arxiv.org/abs/0910.4823); [arXiv:0911.4750](https://arxiv.org/abs/0911.4750).
- [16] D. F. V. James, P. G. Kwiat, W. J. Munro, and A. G. White, *Phys. Rev. A* **64**, 052312 (2001).
- [17] Y. H. Kim, *Phys. Rev. A* **67**, 040301(R) (2003).